ARMY RESEARCH LABORATORY

Gap Formations in Simulations of SHPB Tests on Elastic Materials Soft in Shear

by M. N. Raftenberg and M. J. Scheidler

ARL-RP-272 **September 2009**

A reprint from *Shock Compression of Condensed Matter – 2009, Proceedings of the Conference of the American Physics Society Topical Group on Shock Compression of Condensed Matter,* Nashville, TN, 28 June–3 July 2009.

NOTICES

Disclaimers

The findings in this report are not to be construed as an official Department of the Army position unless so designated by other authorized documents.

Citation of manufacturer's or trade names does not constitute an official endorsement or approval of the use thereof.

Destroy this report when it is no longer needed. Do not return it to the originator.

Army Research Laboratory
Aberdeen Proving Ground, MD 21005-5066

ARL-RP-272 **September 2009**

Gap Formations in Simulations of SHPB Tests on Elastic Materials Soft in Shear

M. N. Raftenberg and M. J. Scheidler
Weapons and Materials Research Directorate, ARL

A reprint from *Shock Compression of Condensed Matter – 2009, Proceedings of the Conference of the American Physics Society Topical Group on Shock Compression of Condensed Matter,* Nashville, TN, 28 June–3 July 2009.

REPORT DOCUMENTATION PAGE

Form Approved
OMB No. 0704-0188

1. REPORT DATE *(DD-MM-YYYY)*	2. REPORT TYPE	3. DATES COVERED (From - To)
September 2009	Reprint	July 2008–July 2009

4. TITLE AND SUBTITLE
Gap Formations in Simulations of SHPB Tests on Elastic Materials Soft in Shear

5a. CONTRACT NUMBER

5b. GRANT NUMBER

5c. PROGRAM ELEMENT NUMBER

6. AUTHOR(S)
M. N. Raftenberg and M. J. Scheidler

5d. PROJECT NUMBER
622618H80

5e. TASK NUMBER

5f. WORK UNIT NUMBER

7. PERFORMING ORGANIZATION NAME(S) AND ADDRESS(ES)
U.S. Army Research Laboratory
ATTN: RDRL-WMT-D
Aberdeen Proving Ground, MD 21005-5066

8. PERFORMING ORGANIZATION REPORT NUMBER
ARL-RP-272

9. SPONSORING/MONITORING AGENCY NAME(S) AND ADDRESS(ES)

10. SPONSOR/MONITOR'S ACRONYM(S)

11. SPONSOR/MONITOR'S REPORT NUMBER(S)

12. DISTRIBUTION/AVAILABILITY STATEMENT
Approved for public release; distribution is unlimited.

13. SUPPLEMENTARY NOTES
A reprint from *Shock Compression of Condensed Matter – 2009, Proceedings of the Conference of the American Physics Society Topical Group on Shock Compression of Condensed Matter*, Nashville, TN, 28 June–3 July 2009.

14. ABSTRACT

The LS-DYNA code was applied to split Hopkinson pressure bar tests on a material at least two orders of magnitude stiffer in dilatation than in shear. Two constitutive models were applied, linear elasticity and a compressible form of Mooney-Rivlin elasticity. The latter was fitted to data from ballistic gelatin. The incident and transmission bars were aluminum. The nominal strain rate was 2500/s. Gaps appeared at the interfaces between the specimen and both bars. Unloading of the specimen and bars accompanied these gaps. The input-velocity rise time was varied to observe pulse shaping effects. Mesh sensitivity and contact-parameter sensitivity studies were performed.

15. SUBJECT TERMS
split Hopkinson pressure bar, ballistic gelatin, LS-DYNA, interfacial gaps

16. SECURITY CLASSIFICATION OF:			17. LIMITATION OF ABSTRACT	18. NUMBER OF PAGES	19a. NAME OF RESPONSIBLE PERSON
a. REPORT	b. ABSTRACT	c. THIS PAGE			Martin N. Raftenberg
Unclassified	Unclassified	Unclassified	UU	12	19b. TELEPHONE NUMBER (*Include area code*) 410-278-3684

GAP FORMATIONS IN SIMULATIONS OF SHPB TESTS ON ELASTIC MATERIALS SOFT IN SHEAR

M. N. Raftenberg[1], **M. J. Scheidler**[1]

[1]*Impact Physics Branch, U.S. Army Research Laboratory, Aberdeen Proving Ground MD 21005*

Abstract. The LS-DYNA code was applied to split Hopkinson pressure bar tests on a material at least two orders of magnitude stiffer in dilatation than in shear. Two constitutive models were applied, linear elasticity and a compressible form of Mooney-Rivlin elasticity. The latter was fitted to data from ballistic gelatin. The incident and transmission bars were aluminum. The nominal strain rate was 2500/s. Gaps appeared at the interfaces between the specimen and both bars. Unloading of the specimen and bars accompanied these gaps. The input-velocity rise time was varied to observe pulse shaping effects. Mesh sensitivity and contact-parameter sensitivity studies were performed.

Keywords: split Hopkinson pressure bar, ballistic gelatin, LS-DYNA, interfacial gaps.
PACS: 62.20.D-, 83.60.-a, 83.60.Uv.

INTRODUCTION

The LS-DYNA code [1] was applied to axisymmetric finite-element simulations of split Hopkinson pressure bar (SHPB) tests on a material much less stiff in shear than in dilatation. This class has relevance to various biological materials and to their simulant, ballistic gelatin. The measurement of high-rate properties for such materials is challenging due to their small wave speeds and impedances. A recent report has documented progress in extending the SHPB technique to ballistic gelatin [2]. The original motivation for our computations was to study the degree to which equilibrium was achieved in these experiments. Both linear elasticity and a compressible form of Mooney-Rivlin elasticity were applied to the specimen. An unanticipated finding was the occurrence of separation gaps between the specimen and the aluminum bars and accompanying unloading of the specimen and bars.

THE MODEL

Constitutive Modeling

The aluminum incident and transmission bars were modeled with linear elasticity. Aluminum was assigned the density of 2700 kg/m^3, Young's modulus of 68 GPa, and Poisson's ratio of 0.33.

The specimen was modeled as elastic with an initial density of 1000 kg/m^3. First a compressible generalization of Mooney-Rivlin hyperelasticity ("CMR"), LS-DYNA model 27 [1,3], was applied. The strain energy per volume, W, is related to the three invariants of the right Cauchy-Green tensor, I, II, and III, by

$$W = A(I-3) + B(II-3) + C(III^{-2}-1) + D(III-1)^2 \quad (1)$$

Here, A, B, C , and D are constants related by

$$C = \frac{A}{2} + B \quad (2)$$

$$D = \frac{A(5\nu - 2) + B(11\nu - 5)}{2(1 - 2\nu)} \qquad (3)$$

and ν is Poisson's ratio.

In calculations applying CMR, A and B were set to 12 and 28 kPa, respectively, in order to produce a stiffness intermediate between uniaxial-stress measurements reported in [2] at strain rates of 1/s and 2500/s. Constant ν was set to 0.49999 to produce an initial bulk modulus four orders of magnitude greater than the shear modulus. In calculations applying linear elasticity, Young's modulus was fixed at 430 kPa and Poisson's ratio ν was varied.

Geometry and Meshing

All simulations were 2D axisymmetric. The specimen's initial thickness and radius were 1.45 and 6.35 mm, respectively, the dimensions used in [2]. The bars had a 12.8-mm radius. The incident and transmission bars had lengths of 768 and 256 mm, respectively, or 30 and 10 times their diameter, respectively.

All finite element meshes were composed of four-node quadrilaterals. In the bars, all elements were 100-μm squares. In most of our calculations, the specimen's elements were initially rectangular, having radial and axial dimensions of 25 and 50 μm, respectively. Several calculations were performed with different specimen meshes to observe convergence.

Boundary Conditions

Interactions between the specimen and the bars was governed by a penalty-based contact algorithm, LS-DYNA's "2D Automatic Surface-to-Surface" [1,3]. The algorithm's key parameters are SFACT, a scale factor applied to the penalty force stiffness, and VDC, a viscous damping coefficient in percent of critical damping. The defaults of 1 and 10, respectively, were used in all calculations from which results are shown. Parameters SFACT and VDC were varied in other calculations to examine convergence.

The outer radii of the bars and specimen were stress-free. At the input end of the incident bar, axial velocity was prescribed in the form

$$v_z(t) = \begin{cases} v_0 \cdot \dfrac{t}{t_R} & ; \quad 0 \le t < t_R \\ v_0 & ; \quad t \ge t_R \end{cases} \qquad (4)$$

Here, t is time. Rise time t_R was assigned the values 1 and 25 μs to explore effects of pulse shaping. The value 1.81 m/s was applied to v_0 to achieve a nominal strain rate of 2500/s across the specimen. At the far end of the transmission bar, LS-DYNA's "2D Non-Reflecting" boundary condition [1,3] was applied.

Results and Discussion

Calculations with Compressible Mooney-Rivlin

Let $\Delta_{S\text{-}IB}$ denote the axial separation between the specimen and the incident bar at the centerline, $r = 0$. Let $\Delta_{S\text{-}TB}$ denote the axial separation between the specimen and the transmission bar at $r = 0$. Let λ_z denote the specimen's nominal axial stretch ratio, defined as the distance between the incident and transmission bars at $r = 0$. Figure 1 shows results for these quantities vs. time for $t_R = 1$ μs. At $r = 0$, the longitudinal wave in the incident bar arrived at the specimen interface at 126 μs. By 165 μs, the specimen has pulled away from the incident bar, thereby producing a non-zero $\Delta_{S\text{-}IB}$. By 166 μs, the specimen has begun to lag behind the transmission bar, leading to a non-zero $\Delta_{S\text{-}TB}$. Three distinct intervals can be discerned in Fig. 1. The first interval occurs between 165 and about 280 μs and corresponds to a λ_z range of 0.97 and 0.68. In this interval $\Delta_{S\text{-}IB}$ remains non-zero and attains a 38-μm peak value, and $\Delta_{S\text{-}TB}$ is intermittently non-zero and attains a peak of 3 μm. Both gaps remain closed in the brief second interval. The third interval extends from about 185 to 325 μs and corresponds to a range of 0.67 to 0.57 for λ_z. During the third interval, $\Delta_{S\text{-}IB}$ and $\Delta_{S\text{-}TB}$ are of similar amplitudes and attain peak values of 43 and 39 μm, respectively.

Figure 2 compares $\Delta_{S\text{-}IB}$ for $t_R = 1$ and 25 μs. Pulse shaping has decreased the size of the gaps. The peak value in Fig. 2 has decreased from 43 to 3 μm. However, even these small-amplitude gaps

were accompanied by stress unloading in the specimen and in the bars. This can be seen in Fig. 3, which compares $\Delta_{S\text{-}TB}$ with axial stress σ_{zz} in the specimen element and in the bar element closest to the S-TB interface at $r = 0$ for $t_R = 25$ μs. The initial compressive pulses that arrived in both bars at about 150 μs were reduced to zero when the gap, of only 1.2 μm amplitude, formed at 184 μs. Thereafter, intermittent gap closings were accompanied by resumptions in compressive stress.

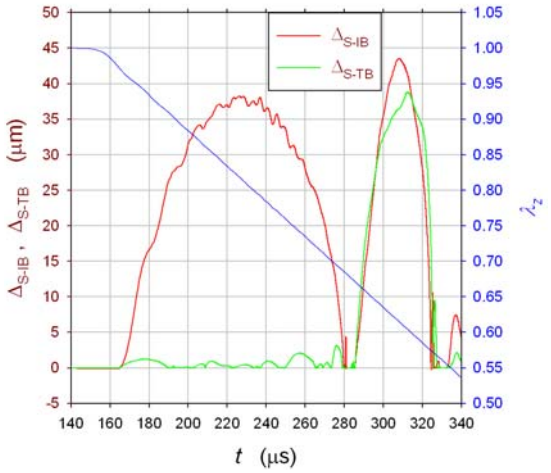

Figure 1. Gap amplitudes at the S-IB and S-TB interfaces at $r = 0$ and nominal axial stretch ratio vs. time for Compressible Mooney-Rivlin and $t_R = 1$ μs.

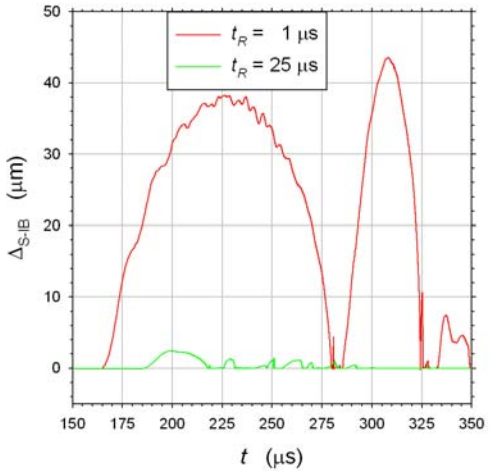

FIGURE 2. Gap amplitude at the S-IB interface at $r = 0$ vs. time for Compressible Mooney-Rivlin and $t_R = 1$ and 25 μs.

Such unloading in the bar and specimen as observed in Fig. 3 would invalidate the processing procedure usually applied to SHPB data [4]. Axial stress σ_{zz} is usually assumed to be uniform throughout the specimen and is related to the strain ε_{zz} measured on the outer surface of the transmission bar by

$$\sigma_{zz} = \frac{A_B}{A_S} E \varepsilon_{zz} \tag{5}$$

Here, E is Young's modulus of the bars, and A_B and A_S are the cross-sectional areas of the bars and specimen, respectively. However, the presence of the S-TB gap implies that the contact area is less than the entire cross-sectional area as assumed in the derivation of eq. 5. Also, the surface unloading in Fig. 3 propagates into the interior of the specimen and delays the occurrence of a uniform state of stress.

The $\Delta_{S\text{-}IB}$ and $\Delta_{S\text{-}TB}$ values in Figs. 1, 2 and 3 are small relative to each specimen-element's initial axial×radial dimensions of 25×50 μm. Two other element sizes, 50×100 and 12.5×12.5 μm, were therefore applied to study convergence. Figure 4 shows that, for $t_R = 1$ μs, the $\Delta_{S\text{-}IB}$ results have substantially converged during the first interval, between 165 and 280 μs. Mesh convergence has not been demonstrated for many aspects of the results, but the degree of convergence in Fig. 4 supports the existence of the gap phenomenon.

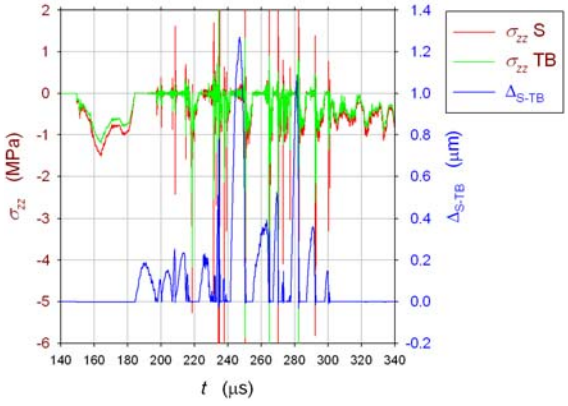

Figure 3. Axial stresses on both sides of the S-TB interface and gap amplitude at this interface, all at $r = 0$, vs. time for Compressible Mooney-Rivlin and $t_R = 25$μs.

Convergence with respect to the contact parameters was also studied. The simulation with t_R = 1 μs was repeated with SFACT equal to 0.1 and 10 and with VDC equal to 20. Again, substantial convergence was demonstrated for $\Delta_{S\text{-}IB}$ during the first interval, but other aspects of the solution have not fully converged.

Calculations with Linear Elasticity

We applied linear elasticity to the specimen. Young's modulus was fixed at 430 kPa and Poisson's ratio ν was varied. The results for $\Delta_{S\text{-}IB}$ for t_R = 25 μs are shown in Fig. 5. This corresponds to a nearly fixed shear modulus and varied bulk modulus. No gaps were detected at either interface for a ν of 0.48 or less. The largest peak values (with respect to time) for both $\Delta_{S\text{-}IB}$ and $\Delta_{S\text{-}TB}$ were observed with a ν of 0.4990. Peak values diminished when ν was increased further.

Figure 6 contains a mesh plot for ν = 0.49900 at 286 μs. The values for both $\Delta_{S\text{-}IB}$ and $\Delta_{S\text{-}TB}$ exceed the specimen element dimensions. This observation further supports the assessment that the gap phenomenon is not entirely an artifact of meshing.

CONCLUSIONS

We have not found any explicit mention of the gap phenomenon in the SHPB literature, either experimental or computational. Each of our specimen materials had a shear modulus much smaller than its bulk modulus, an impedance much less than that of the aluminum bars, and was purely elastic. It is not yet clear which of these properties was/were essential in producing the gaps.

REFERENCES

1. Livermore Software Technology Corporation, LS-DYNA Keyword User's Manual, Volume II, Version 971, May 2007.
2. Moy, P., et al., "Dynamic Response of an Alternative Tissue Simulant Physically Associating Gels (PAG)", ARL report, ARL-RP-136, 2006.
3. Hallquist, J. O., LS-DYNA Theory Manual, 2006.
4. Gray, G. T., III, "Classic Split-Hopkinson Pressure Bar Testing", ASM Handbook V. 8, 2000, 462-476.

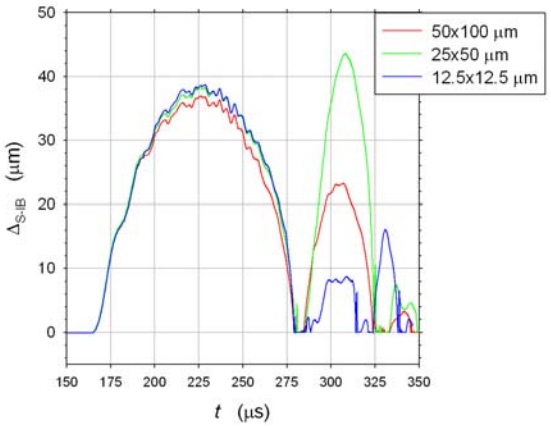

Figure 4. Gap amplitude at the S-IB interface at r = 0 vs. time for Compressible Mooney-Rivlin, t_R = 1 μs, and three different specimen meshes.

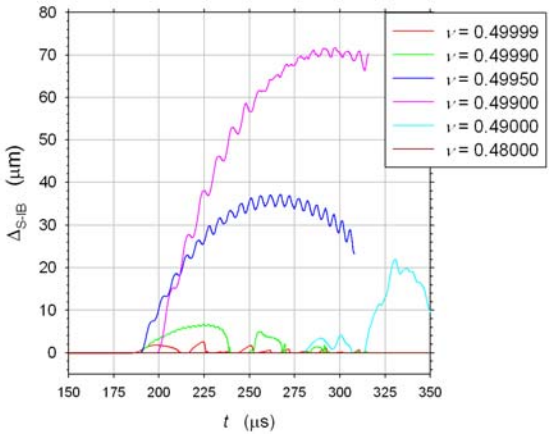

Figure 5. Gap amplitude at the S-IB interface at r = 0 vs. time for t_R = 25 μs and linear elastic specimens with a Young's modulus of 430 kPa and various Poisson ratios.

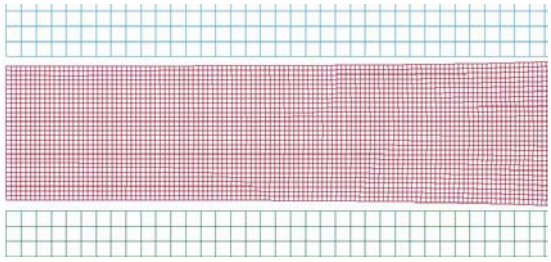

Figure 6. Mesh plot at 286 μs for the linear elastic specimen with a Poisson's ratio of 0.49900, a Young's modulus of 430 kPa and for t_R = 25 μs. The centerline is on the left and the incident bar is at the bottom.

NO. OF
COPIES ORGANIZATION

1 (PDF only) DEFENSE TECHNICAL INFORMATION CTR
DTIC OCA
8725 JOHN J KINGMAN RD
STE 0944
FORT BELVOIR VA 22060-6218

1 DIRECTOR
US ARMY RESEARCH LAB
IMNE ALC HRR
2800 POWDER MILL RD
ADELPHI MD 20783-1197

1 DIRECTOR
US ARMY RESEARCH LAB
RDRL CIM L
2800 POWDER MILL RD
ADELPHI MD 20783-1197

1 DIRECTOR
US ARMY RESEARCH LAB
RDRL CIM P
2800 POWDER MILL RD
ADELPHI MD 20783-1197

ABERDEEN PROVING GROUND

1 DIR USARL
RDRL CIM G (BLDG 4600)

NO. OF COPIES ORGANIZATION

3 INSTITUTE FOR ADVANCED TECH
S BLESS
S SATAPATHY
S LEVINSON
3925 WEST BRAKER ST
STE 400
AUSTIN TX 78759-5316

3 SOUTHWEST RSRCH INST
C A ANDERSON
J WALKER
K DANNEMANN
6220 CULEBRA RD
DRAWER 28510
SAN ANTONIO TX 78228-0510

4 SOUTHWEST RSRCH INST
G JOHNSON
T HOLMQUIST
S BEISSEL
C GERLACH
5353 WAYZATA BLVD
MINNEAPOLIS MN 55416-1340

1 INTERNATIONAL RSRCH ASSOC
D ORPHAL
4450 BLACK AVE STE E
PLEASANTON CA 94566-6145

2 JOHNS HOPKINS UNIV
MECHL ENGRG
K T RAMESH
K HEMKER
223 LATROBE HALL
3400 N CHARLES ST
BALTIMORE MD 21218-2682

1 JOHNS HOPKINS UNIV
CIVIL ENGRG
L GRAHAM-BRADY
210 LATROBE HALL
3400 N CHARLES ST
BALTIMORE MD 21218-2682

1 LIVERMORE SOFTWARE TECHLGY CORP
M JENSEN
7374 LAS POSITAS RD
LIVERMORE CA 94550

NO. OF COPIES ORGANIZATION

1 UNIVERSITY OF ALABAMA
AT BIRMINGHAM
MECHANICAL ENGRG
D LITTLEFIELD
HOEN ENGR BLDG
1530 3RD AVE S
BIRMINGHAM AL 35294-4440

1 PURDUE UNIVERSITY
ARNTCS & ASTRONAUTICS
W CHEN
701 W STADIUM AVE
W LAFAYETTE IN 47907-2045

1 UNIVERSITY OF MISSISSIPPI
MECHANICAL ENGRG
A RAJENDRAN
201 CARRIER HALL
UNIVERSITY MS 38677

2 WAYNE STATE UNIVERSITY
BIOMEDICAL ENGRG
C BIR
K-H YANG
818 W HANCOCK
DETROIT MI 48201

3 UNIVERSITY OF CALIFORNIA
SAN DIEGO
MECHL AND ARSPC ENGRG
M MEYER
S NEMAT-NASSER
V NESTERENKO
9500 GILMAN DR
LA JOLLA CA 92093-0411

1 UNIVERSITY OF UTAH
MECHANICAL ENGRG
R BRANNON
50 S CENTRAL CAMPUS DR
SALT LAKE CITY UT 84112

1 BROWN UNIVERSITY
ENGRG DIV
R CLIFTON
182 HOPE ST
PROVIDENCE RI 02912

2 AIR FORCE RSRCH LAB
RWMW
J L JORDAN
L CHHABILDAS
101 WEST EGLIN BLVD
EGLIN AFB FL 32542

NO. OF COPIES ORGANIZATION

4 SANDIA NATIONAL LABS
M R BAER MS 0836
S SILLING MS 1322
E S HERTEL MS 1185
P A TAYLOR MS 1160
PO BOX 5800
ALBUQUERQUE NM 97185

1 SANDIA NATIONAL LABS
T J VOGLER
PO BOX 969
LIVERMORE CA 94551-0969

7 LOS ALAMOS NATIONAL LAB
B CLEMENTS
E N BROWN
E MAS
T MASON
P RAE
D DATTELBAUM
M MURPHY
PO BOX 1663
LOS ALAMOS NM 87545

1 LAWRENCE LIVERMORE
NATIONAL
LAB
D GOTO
PO BOX 808
LIVERMORE CA 94551-0808

1 APPLIED RSRCH ASSOC
SOUTHWEST DIV
D E GRADY
4300 SAN MATEO BLVD NE
ALBUQUERQUE NM 87110

ABERDEEN PROVING GROUND

42 DIR USARL
RDRL CIH C
J CAZAMIAS
P CHUNG
D GROVE
RDRL WM
J SMITH
RDRL WMM B
M BERMAN
D HOPKINS
A FRYDMAN
G GAZONAS
M MINNICINO
B POWERS

NO. OF COPIES ORGANIZATION

C RANDOW
J SOUTH
RDRL WMM D
E CHIN
C FOUNTZOULAS
RDRL WMS
T JONES
RDRL WMT
P BAKER
RDRL WMT A
E HORWATH
J HOUSKAMP
C KRAUTHAUSER
S SCHOENFELD
RDRL WMT
C HOPPEL
RDRL WMT B
R BITTING
D FOX
R GUPTA
S KUKUCK
RDRL WMT C
T BJERKE
M FERMEN-COKER
S SCHRAML
K KIMSEY
D SCHEFFLER
RDRL WMT D
S BILYK
D CASEM
J CLAYTON
N GNIAZDOWSKI
Y HUANG
M KIM
R KRAFT
B LOVE
M RAFTENBERG
M SCHEIDLER
T WEERASOORIYA
K ZIEGLER

INTENTIONALLY LEFT BLANK.